

# Two- and Three-Body Charmless $B$ Decays at BaBar

S. Stracka on behalf of the BaBar Collaboration

Università degli Studi di Milano and INFN, Sezione di Milano - I-20133 Milano, Italy

We report recent measurements of rare charmless  $B$  decays performed by BaBar. The results are based on the final BaBar dataset of  $424 \text{ fb}^{-1}$  collected at the PEP-II  $B$ -factory based at the SLAC National Accelerator Laboratory.

## 1. Introduction

The study of rare  $B$  decays is a key ingredient to meet two of the main goals of the  $B$ -factories: assessing the validity of the Cabibbo-Kobayashi-Maskawa (CKM) picture of  $CP$ -violation [1] by precisely measuring the elements of the Unitarity Triangle (UT), and searching for hints of New Physics (NP), or otherwise constraining NP scenarios, in processes which are suppressed in the Standard Model (SM). In loop processes, in particular, NP at some higher energy scale may manifest itself in the low energy effective theory as new couplings, such as those introduced by new very massive virtual particles in the loop [2]. In NP searches hadronic uncertainties can play a major role, especially for branching fraction measurements. Many theoretical uncertainties cancel in ratios of amplitudes, and most NP probes are therefore of this kind.

In the following sections we report recent measurements, performed by the BaBar Collaboration, that are relevant to NP searches in charmless hadronic  $B$  decays. In Sec. 2 we report the 2008 update of the time-dependent analyses of  $B^0 \rightarrow \eta' K^0$  and  $B^0 \rightarrow \omega K_S$  decays. In Sec. 3 we describe the search for  $B$  decays to the three-body final states  $PK_S K_S$ , where  $P = \eta, \eta', \pi^0$ . The Dalitz Plot analysis of  $B \rightarrow K_S \pi \pi$  decays is reported in Sec. 4. These measurements are related to the CKM angle  $\beta$ , which is experimentally accessible through the interference between the direct decay of the  $B$  meson to a  $CP$  eigenstate and the decay after  $B^0 \bar{B}^0$  mixing. This interference affects the time evolution of the decay.

In the time-dependent analyses of  $B$  decays, one of the two  $B$  mesons produced in  $e^+e^- \rightarrow \Upsilon(4S) \rightarrow B\bar{B}$  events is fully reconstructed according to the final state  $f$  of interest. The flavor and the decay vertex position for the other  $B$  in the event ( $B_{tag}$ ) are identified from its decay products. The proper time difference between the two  $B$  mesons is:

$$f(\Delta t) = \frac{e^{-|\Delta t|/\tau}}{4\tau} \{1 + q[-\eta_f S_f \sin(\Delta m_d \Delta t) - C_f \cos(\Delta m_d \Delta t)]\}, \quad (1)$$

where  $\eta_f$  is the  $CP$  eigenvalue of the final state  $f$ ,  $q = +1(-1)$  if the  $B_{tag}$  decays as a  $B^0$  ( $\bar{B}^0$ ),

$\tau = (1.536 \pm 0.014) \text{ ps}$  [3] is the mean  $B$  lifetime, and  $\Delta m_d = (0.502 \pm 0.007) \text{ ps}^{-1}$  is the  $B^0 - \bar{B}^0$  mixing frequency [3].

The angle  $\beta$  can be determined very accurately and with small theoretical uncertainties from the analysis of the decay rate asymmetries in  $b \rightarrow c\bar{c}s$  decays, and is related in a simple way to the parameter  $S_{cc}$  in Eq. 1:

$$S_{cc} = -\eta_f \sin 2\beta. \quad (2)$$

The current world average is  $S_{cc} = 0.67 \pm 0.02$  [4].

A parameter  $S_{qq} = -\eta_{CP} \sin 2\beta_{\text{eff}}$  (where  $\beta_{\text{eff}}$  denotes an effective value of  $\beta$ ) can also be extracted from penguin (loop) dominated  $b \rightarrow q\bar{q}s$  decays. These decays may receive contributions from NP effects that can lead to measurable differences  $\Delta S \equiv S_{qq} - S_{cc}$ . In some NP scenario, deviations can be  $\approx O(1)$  [5]. A background to  $\Delta S$  measurements as a tool for NP searches is represented by the CKM suppressed tree contributions, which may introduce shifts in the parameter  $S$ . The SM effect is predicted in most models to be a positive shift in  $\Delta S$  [6]. The size of this shift is related to the ratio of tree to penguin amplitudes, which depends on the decay mode. Theoretical estimates for this ratio are affected by large uncertainties for most decay modes, with the exception of the  $K_S K_S K^0$ ,  $\phi K^0$ , and  $\eta' K^0$  modes.

The updated measurement of the direct  $CP$ -violation parameter for  $B \rightarrow K^+ \pi^-$  is reported in Sec. 5.  $B \rightarrow K\pi$  transitions receive contributions from tree, color suppressed tree, gluonic penguin (loop), and electroweak penguin contributions. Among these amplitudes, the dominant contribution is represented by the gluonic penguin. The electroweak penguin and the color suppressed tree amplitudes are expected to be small in the SM, and the direct  $CP$ -violation parameter for  $K^+ \pi^-$  decays should be equal to that for  $K^+ \pi^0$  decays. The rates and direct  $CP$ -violating asymmetries in the  $K\pi$  system reveal puzzling features, that might be indications of NP.

## 2. $B^0 \rightarrow \eta' K^0$ and $B^0 \rightarrow \omega K_S$

The BaBar Collaboration has updated the measurement of  $CP$ -violating asymmetries in  $B$  decays to

$\eta'K^0$  and  $\omega K_S$  using the final dataset corresponding to 465 million  $B\bar{B}$  pairs [7].

The  $\eta'K^0$  channel provides the most precise measurement of  $S$  in a penguin dominated mode. The time-dependent analysis of the  $B \rightarrow \eta'K^0$  decays is performed on about 2500 signal events, corresponding to a branching fraction of  $\approx 65 \times 10^{-6}$ . The resulting decay rate distributions are shown in Fig. 1. Both  $\eta'K_S$  and  $\eta'K_L$  modes are analyzed, and the results are combined in scans of  $-\ln \mathcal{L}$ , taking into account the different intrinsic  $CP$  parity. With respect to the previous measurement, the analysis relies on about 20% more data, improved track reconstruction, and reconstruction of an additional  $\eta'$  decay channel in  $\eta'K_L$  analysis. The results for the  $CP$ -violation parameters  $S$  and  $C$  in this decay mode are [7]:

$$S_{\eta'K^0} = 0.57 \pm 0.08 \pm 0.02 \quad (3)$$

$$C_{\eta'K^0} = -0.08 \pm 0.06 \pm 0.02, \quad (4)$$

where the first error is statistical and the second systematic. The uncertainties on  $S$  and  $C$  have decreased by about 20% and 25%, respectively, and are still statistically limited. The observed discrepancy between  $S_{cc}$  and  $S_{\eta'K^0}$  is not significant. Since this is one of the theoretically cleanest modes, the study of decay rate asymmetries in  $B^0 \rightarrow \eta'K^0$  decays is a benchmark analysis for a Super  $B$  factory [8].

In the  $B^0 \rightarrow \omega K_S$  channel the tree to penguin ratio is not necessarily small. If the two contributions are comparable in size they can lead to a non-zero direct  $CP$  parameter. For the  $\omega K_S$  channel,  $B$  daughters are reconstructed in the main decay modes,  $\omega \rightarrow \pi^+\pi^-\pi^0$  and  $K_S \rightarrow \pi^+\pi^-$ . The  $\omega$  mass and angular variables are included in the fit. The signal yield for the  $\omega K_S$  channel is much lower ( $N = 163$ ) than that for the  $\eta'K^0$  channel, and the measurement of  $S$  and  $C$  is therefore less precise. The extracted values for these parameters are [7]:

$$S_{\omega K_S} = 0.55^{+0.26}_{-0.29} \pm 0.02 \quad (5)$$

$$C_{\omega K_S} = -0.52^{+0.22}_{-0.20} \pm 0.03 \quad (6)$$

The central value of  $C$  is of potential interest as it differs from 0 by more than  $2\sigma$ , but more statistics than that collected at the  $B$ -factories is needed to further investigate direct  $CP$ -violation in this decay.

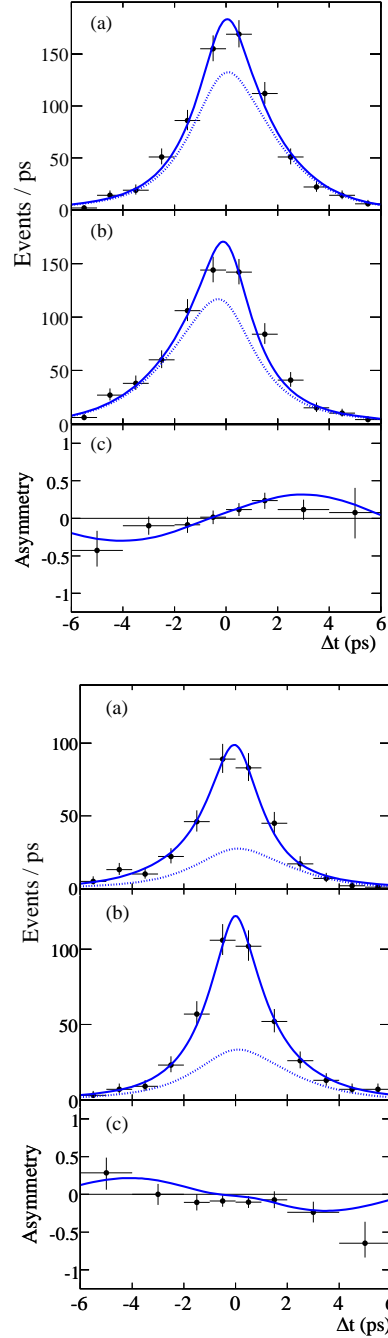


Figure 1: Data and model projections for  $\eta'K_S$  (top) and  $\eta'K_L$  (bottom) onto  $\Delta t$  for (a)  $B^0$  and (b)  $\bar{B}^0$  tags. Points with error bars represent the data: the solid (dotted) line displays the total fit function (total signal). In (c) we show the raw asymmetry,  $(N_{B^0} - N_{\bar{B}^0})/(N_{B^0} + N_{\bar{B}^0})$ : the solid line represents the fit function [7].

### 3. $B^0 \rightarrow X^0 X^0 P^0$

Decays to  $CP$ -eigenstate final states with three  $CP$  eigenstate particles, two of which are equal, allow the measurement of  $\beta_{\text{eff}}$  from time-dependent  $CP$ -asymmetries. Since the  $CP$ -eigenvalue is independent of the intermediate resonant structure, there is no need for an isospin or Dalitz Plot analysis to separate the different resonant contributions [9]. BaBar has searched for these decay channels in  $426 \text{ fb}^{-1}$  data [10]. A maximum likelihood fit to kinematical and topological variables is performed but no evidence of signal is found (see Table I), and yields are too small to allow a time-dependent analysis.

Table I Branching fraction results and upper limits at 90% confidence level (CL) for  $B^0 \rightarrow X^0 X^0 P^0$  channels [10].

Mode	$\mathcal{B}(\times 10^{-6})$	90% CL UL ( $\times 10^{-6}$ )
$\pi^0 K_S K_S$	$2.7_{-3.7}^{+4.2} \pm 0.6$	9
$\eta K_S K_S$	$2.7_{-3.8}^{+4.7} \pm 1.2$	10
$\eta' K_S K_S$	$2.7_{-6.5}^{+8.0} \pm 3.4$	20

### 4. $B^0 \rightarrow K_S \pi^+ \pi^-$

The  $S$  parameter can be extracted from a time-dependent Dalitz Plot analysis of  $B \rightarrow K_S \pi \pi$  transitions. BaBar has performed an analysis of this decay using a data sample of 383 million  $B\bar{B}$  pairs [11].

The decay amplitude can be parameterized as a function of two Mandelstam-like variables  $s_+ \equiv m_{K_S^0 \pi^+}^2$  and  $s_- \equiv m_{K_S^0 \pi^-}^2$  according to the isobar model:

$$A(s_+, s_-) = \sum_{j=1}^N |c_j| e^{-i\phi_j} \times R_j(m) X_L(|\vec{p}^*| r') X_L(|\vec{q}| r) T_j(L, \vec{p}, \vec{q}). \quad (7)$$

Here the complex coefficients  $|c_j|$  and  $e^{-i\phi_j}$  are the relative magnitude and phase for the channel  $j$ ,  $R_j(m)$  is the lineshape term,  $X_L$  are Blatt-Weisskopf barrier factors [12],  $T_j$  is the angular distribution,  $\vec{p}$  is the momentum of the bachelor particle,  $\vec{q}$  is the momentum of one of the resonance daughters,  $L$  is the orbital angular momentum between  $\vec{p}$  and the resonance momentum, and a star denotes the  $B$ -meson rest frame. The signal model includes both  $\pi\pi$  ( $\rho(770)$ ,  $f_0(980)$ ,  $f_2(1270)$ ,  $f_X(1300)$ ,  $\chi_{c0}$ ) and  $K\pi$  ( $K^*(892)$ ,  $(K\pi)_{S\text{-wave}}$ ) resonances as well as non-resonant contributions, for a total of 15 complex scalar amplitudes.

The choice of  $s_+$  and  $s_-$  as independent variables is impractical because both the signal events and the

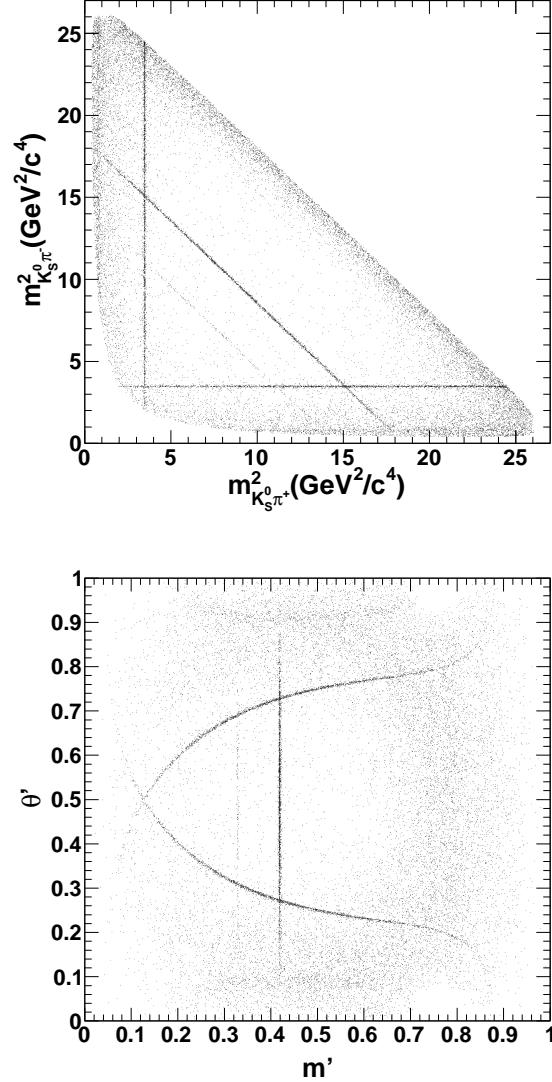


Figure 2: Standard (top) and square (bottom) Dalitz plots of  $B^0 \rightarrow K_S \pi^+ \pi^-$  candidates [11].

combinatorial  $e^+e^- \rightarrow q\bar{q}$  events populate the kinematic boundaries of the Dalitz Plot. The following new coordinates are therefore introduced:

$$m' \equiv \frac{1}{\pi} \arccos \left( 2 \frac{m_0 - m_0^{\min}}{m_0^{\max} - m_0^{\min}} - 1 \right), \quad \theta' \equiv \frac{1}{\pi} \theta_0,$$

where  $m_0$  is the  $\pi^+ \pi^-$  invariant mass,  $m_0^{\max}$  and  $m_0^{\min}$  are the kinematic limits of  $m_0$ , and  $\theta_0$  is the  $\pi^+ \pi^-$  resonance helicity angle. The following transformation is applied,

$$ds_+ ds_- \rightarrow |\det J| dm' d\theta' \quad (8)$$

which defines the square Dalitz Plot shown in Fig. 2.

The distribution of the proper-time difference be-

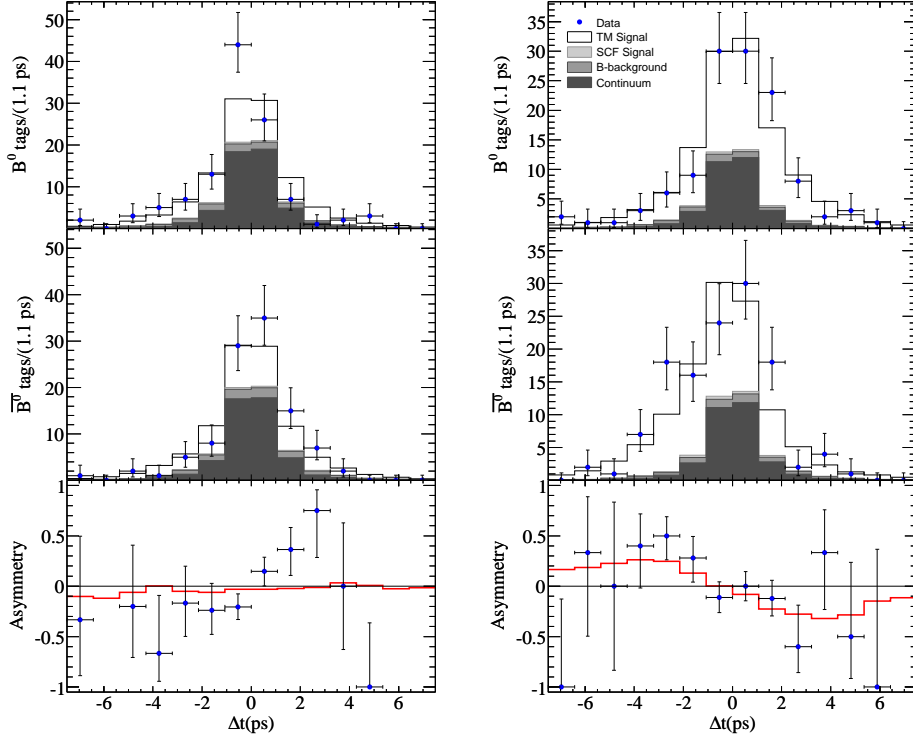


Figure 3: Distributions of  $\Delta t$  when the  $B_{tag}$  is a  $B^0$  (top),  $\bar{B}^0$  (middle), and the derived  $\Delta t$  asymmetry (bottom). Plots on the left (right) hand side, correspond to events in the  $f_0(980)K_S$  ( $\rho(770)^0 K_S$ ) region [11].

tween the two  $B$ -mesons is given by:

$$f(\Delta t) = \frac{e^{-|\Delta t|/\tau}}{\tau} [ |A|^2 + |\bar{A}|^2 \mp (|A|^2 - |\bar{A}|^2) \cos(\Delta m_d \Delta t) \pm \eta_f 2\text{Im}[\bar{A}A^*] \sin(\Delta m_d \Delta t) ],$$

where the  $CP$ -violation parameters are expressed in terms of the amplitudes  $A$  (for  $B$  decays) and  $\bar{A}$  (for  $\bar{B}$  decays). From the results of this analysis for  $B^0$  decays to  $\rho(770)^0 K_S$  and  $f_0(980) K_S$   $CP$ -eigenstates it is possible to calculate  $\beta_{\text{eff}}$  as:

$$\beta_{\text{eff}} = \frac{1}{2} \arg(c_k \bar{c}_k^*). \quad (9)$$

The direct and mixing-induced  $CP$  asymmetries can be calculated as:

$$C_k = \frac{|c_k|^2 - |\bar{c}_k|^2}{|c_k|^2 + |\bar{c}_k|^2} \quad (10)$$

$$S_k = \frac{2\text{Im}(c_k^* \bar{c}_k)}{|c_k|^2 + |\bar{c}_k|^2}. \quad (11)$$

Signal enriched distributions for  $\Delta t$  and  $\Delta t$ -asymmetry for events in the regions of  $\rho(770)$  and  $f_0(980)$  are shown in Fig. 3. Two solutions for the  $S$  and  $C$  parameters are present, almost degenerate in likelihood [11]. For the  $f_0(980) K_S$  channel, there

is an evidence of non-zero  $S$  at about  $3.5\sigma$  significance (see Fig. 4). Including systematic and Dalitz plot model uncertainties, the confidence intervals at 95% confidence level (CL) for the measured value of  $\beta_{\text{eff}}$  in the  $B^0 \rightarrow \rho^0(770) K_S$  and  $B^0 \rightarrow f_0(980) K_S$  channels are [11]:

$$-9^\circ < \beta_{\text{eff}}(\rho^0(770) K_S) < 57^\circ, \quad (12)$$

$$18^\circ < \beta_{\text{eff}}(f_0(980) K_S) < 76^\circ \quad (13)$$

These measurements are consistent with the SM.

The analysis of  $B^0 \rightarrow K_S \pi^+ \pi^-$  decays provides further non-trivial constraints on the  $\rho - \eta$  plane (CKM angle  $\gamma$ ). In particular, the phase difference between isobar amplitudes for  $B^0$  and  $\bar{B}^0$  decays to  $K^*(892)^+ \pi^-$  and  $(K\pi)_{S-wave}^+ \pi^-$

$$\Delta\phi_{K^* \pi} \equiv \arg c_{K^*(892)^+ \pi^-} - \arg c_{K^*(892)^- \pi^+}$$

$$\Delta\phi_{(K\pi)_S \pi} \equiv \arg c_{(K\pi)_S^+ \pi^-} - \arg c_{(K\pi)_S^- \pi^+}$$

can be used to extract information about  $\gamma$  [13]. The one-dimensional scans for  $\Delta\phi_{K^* \pi}$  and  $\Delta\phi_{(K\pi)_S \pi}$  are presented in Fig. 5. Due to the small overlap between the phase space regions accessible to  $B^0$  and  $\bar{B}^0$ , the sensitivity to these phases is limited. The available statistics allows to exclude only small regions at 95% CL. Including systematic effects, the excluded regions

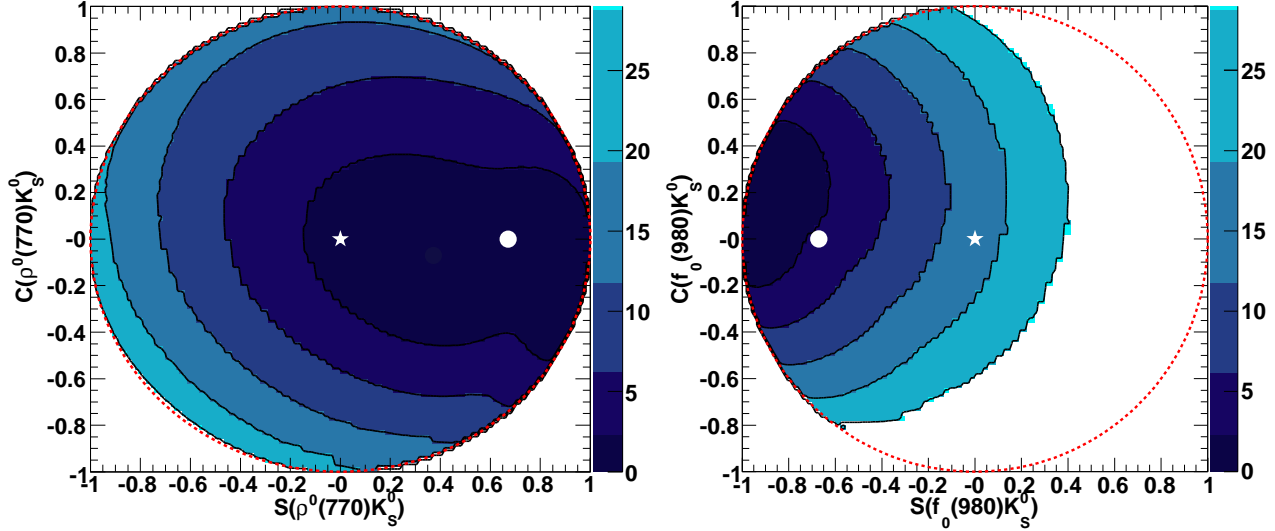


Figure 4: Two-dimensional scans of  $-2\Delta \log \mathcal{L}$  as a function of  $(S, C)$ , for the  $f_0(980)K_S$  (left) and  $\rho(770)^0 K_S$  (right) isobar components [11]. The value  $-2\Delta \log \mathcal{L}$  is computed including systematic uncertainties. Shaded areas, from the darkest to the lightest, represent the one to five standard deviations contours. The  $\bullet$  ( $\star$ ) marks the expectation used on the current world average from  $b \rightarrow c \bar{c} s$  modes [4] (zero point). The dashed circle represents the physical border  $S^2 + C^2 = 1$ .

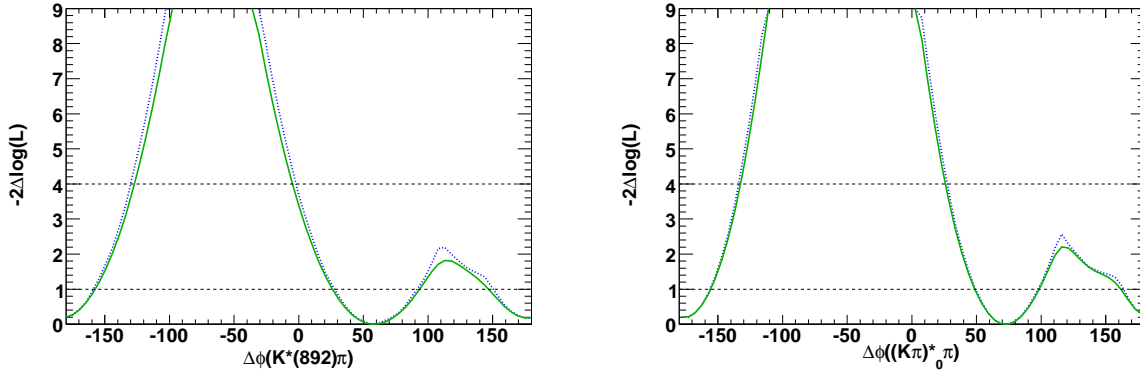


Figure 5: Statistical (dashed line) and total (solid line) scans of  $-2\Delta \log \mathcal{L}$  as a function of the relative phases  $\Delta\Phi(K^*(892)\pi)$  (left) and  $\Delta\Phi((K\pi)_0^*)$  (right) [11]. Horizontal dotted lines mark the one and two standard deviation levels.

are [11]:

$$\begin{aligned} -137^\circ < \Delta\phi_{K^*(892)\pi} < -5^\circ, \\ -132^\circ < \Delta\phi_{(K\pi)_S\pi} < +25^\circ. \end{aligned}$$

## 5. $B^0 \rightarrow K^+\pi^-$

The direct  $CP$  violation  $A_{CP}$  parameter for  $B \rightarrow K^+\pi^-$  has been extracted from a fit to the  $\pi^+\pi^-$ ,  $K^\pm\pi^\mp$ , and  $K^+K^-$  final states, using 467 million  $B\bar{B}$  pairs [14]. Since  $K^+\pi^-$  is a self-tagging mode,  $A_{CP}$

is obtained by simple event-counting:

$$A_{CP} = \frac{N(\bar{B}^0 \rightarrow K^-\pi^+) - N(\bar{B}^0 \rightarrow K^+\pi^-)}{N(\bar{B}^0 \rightarrow K^-\pi^+) + N(\bar{B}^0 \rightarrow K^+\pi^-)}. \quad (14)$$

This analysis yields a  $6.1\sigma$  observation of direct  $CP$  violation,  $A_{CP}(K^+\pi^-) = -0.107 \pm 0.016_{-0.004}^{+0.006}$  [14]. By combining this result with  $A_{CP}(K^+\pi^0)$  and taking the averages with Belle [4], one obtains:

$$A_{CP}(K^+\pi^-) = -0.098_{-0.011}^{+0.012} \quad (15)$$

$$A_{CP}(K^+\pi^0) = +0.050 \pm 0.025. \quad (16)$$

This result corresponds to a  $5\sigma$  deviation from the SM expectation.

Several interpretations have been proposed for this discrepancy. In some models this result is considered as a hint of NP, which might manifest itself with large contributions from electroweak penguins [15]. Standard Model explanations have also been formulated, which involve large color-suppressed trees and nonperturbative effects [16].

## 6. Conclusions

In this paper we have reported recent results on charmless hadronic  $B$  decays obtained by the BaBar experiment. These results can be used to set non-trivial constraints on the Unitarity Triangle, most notably on  $\sin 2\beta$  and  $\gamma$ .

Penguin dominated decays provide several observables that can be used as NP probes. No hint of NP has been found in the channels described in this report, most deviations being within  $2\sigma$  from Standard Model predictions. For the theoretically cleanest modes, the experimental uncertainty on  $\Delta S$  measurements is dominant, thus demanding for more statistics and precision.

In  $B \rightarrow K\pi$  decays a  $5\sigma$  discrepancy with respect to naive Standard Model expectations is observed. The interpretations range from SM explanations to NP effects.

## Acknowledgments

I would like to thank the organizers of DPF 2009 for an interesting conference and my BaBar and PEP-II collaborators for their contributions.

## References

- [1] N. Cabibbo, Phys. Rev. Lett. **10**, 531 (1963); M. Kobayashi and T. Maskawa, Prog. Theor. Phys. **49**, 652 (1973).
- [2] A. Masiero and O. Vives, Annu. Rev. Nucl. Part. Sci. **51**, 161 (2001).
- [3] C. Amsler *et al.* (Particle Data Group), Phys. Lett. B **667**, 1 (2008).
- [4] E. Barberio *et al.* (Heavy Flavor Averaging Group), arXiv:0808.1297 (2008) and online update at <http://www.slac.stanford.edu/xorg/hfag>.
- [5] Y. Grossman and M. P. Worah, Phys. Lett. **B395**, 241 (1997); D. London and A. Soni, Phys. Lett. **B407**, 61 (1997); M. Ciuchini *et al.*, Phys. Rev. Lett. **79**, 978 (1997).
- [6] M. Gronau, Y. Grossman and J. L. Rosner, Phys. Lett. **B579**, 331 (2004); H. Y. Cheng, C. K. Chua and A. Soni, Phys. Rev. D **72**, 014006 (2005); Phys. Rev. D **72**, 094003 (2005); M. Beneke, Phys. Lett. **B620**, 143 (2005); G. Buchalla, G. Hiller, Y. Nir and G. Raz, JHEP 0509, 074 (2005); A. R. Williamson and J. Zupan, Phys. Rev. D **74**, 014003 (2006); H. Li and S. Mishima, Phys. Rev. D **74**, 094020 (2006);
- [7] B. Aubert *et al.* (BaBar Collaboration), Phys. Rev. D **79**, 052003 (2009).
- [8] M. Bona *et al.*, arXiv:0709.0451 [hep-ex] (2007); S. Hashimoto *et al.*, KEK-REPORT-2004-4 (2004).
- [9] T. Gershon and M. Hazumi, Phys. Lett. **B596**, 163 (2004).
- [10] B. Aubert *et al.* (BaBar Collaboration), Phys. Rev. D **80**, 011101 (2009).
- [11] B. Aubert *et al.* (BaBar Collaboration), arXiv:0905.3615 [hep-ex] (2009).
- [12] J. Blatt and V. E. Weisskopf, *Theoretical Nuclear Physics*, J. Wiley (New York), (1952).
- [13] M. Ciuchini, M. Pierini, and L. Silvestrini, Phys. Rev. D **74**, 051301 (2006); M. Gronau, D. Pirjol, A. Soni, and J. Zupan, Phys. Rev. D **75**, 014002 (2007).
- [14] B. Aubert *et al.* (BaBar Collaboration), arXiv:0807.4226 [hep-ex] (2008).
- [15] T. Yoshikawa, Phys. Rev. D **68**, 054023 (2003); S. Mishima and T. Mashikawa, Phys. Rev. D **70**, 094024 (2004); A. J. Buras, R. Fleischer, S. Recksiegel, and F. Schwab, Phys. Rev. Lett. **92**, 101804 (2004); A. J. Buras, R. Fleischer, S. Recksiegel, and F. Schwab, Eur. Phys. Jour. C **45**, 701 (2006); S. Baek and D. London, Phys. Lett. **B653**, 249 (2007); T. Feldmann, M. Jung, and T. Mannel, JHEP 0808, 066 (2008).
- [16] C. W. Chiang, M. Gronau, J. L. Rosner and D. A. Suprun, Phys. Rev. D **70**, 034020 (2004); H. Li, S. Mishima, and A. I. Sanda, Phys. Rev. D **72**, 114005 (2005); M. Ciuchini *et al.*, Phys. Lett. **B674**, 197 (2009).